Journal of Medicinal Chemistry Article

J. Med. Chem. **2010,** *53,* 3065–3074 **3065**
DOI: 10.1021/jm901452y

Virtual Screening for the Identification of Novel Nonsteroidal Glucocorticoid Modulators

Valeria Onnis, Gemma K. Kinsella, Giorgio Carta, William N. Jagoe, Trevor Price, D. Clive Williams, Darren Fayne, and David G. Lloyd*

Molecular Design Group, School of Biochemistry and Immunology, Trinity College Dublin, Dublin 2, Ireland

Received October 1, 2009

In this work, we describe the first application of ligand-based drug design (LBDD) to the derivation of a predictive pharmacophore for the human glucocorticoid receptor (hGR). Creation of a four feature pharmacophore in Catalyst was subsequently validated through a virtual screen of 264000 commercially available compounds. From a selected hit list of 11 diverse compounds, two nonsteroidal molecules demonstrated low micromolar activity against hGR as validated through fluorescence polarization competitive assay. Additionally, these compounds were tested for their trans-repression potential by their ability to inhibit IL-1 induced, IL-6 expression in the human A549 lung epithelial cell line. Co-treatment of A549 with **21** (MDG169) (10 μM) in combination with dexamethasone showed an improved inhibitory effect when compared to dexamethasone alone with the cooperative effect being dependent on the dexamethasone dose. Putative binding orientations in the hGR ligand binding domain crystal structure are presented. These compounds represent novel nonsteroidal hGR modulating scaffolds, rationally identified through ligand-focused computational modeling.

Introduction

The human glucocorticoid receptor (GR[a]) is a steroid hormone-activated transcription factor known to regulate numerous physiological functions of the endocrine and immune systems, including adaptation to physiological or psychological stress.[1] The GR consists of three domains and belongs to the superfamily of nuclear receptors. To date, two isoforms of the receptor have been identified, α and β. The N-Terminal trans-activation domain of the GR includes the activation function domain AF-1 required for transcriptional enhancement and association of the receptor with basal transcription factors. The central, DNA binding domain (DBD) consists of two zinc fingers regions which are critical for receptor dimerization and target binding and also serves as a binding site for the heat shock proteins (HSP). The ligand binding domain (LBD) contains nuclear localization signals, as well as the ligand-dependent activation function domain 2 (AF-2).[2,3]

The first GRα LBD crystal structure was solved by Bledsoe in 2002[4] and consists of 12 helices and four β strands which fold into a three-layer helical domain.[5,6] An analysis of the GR LBD cocrystal structure (PDB: 1M2Z) indicates that the steroidal A ring of dexamethazone (DEX) is positioned adjacent to β strands 1 and 2 and the D ring is close to helix 12. A number of hydrogen bonds (HBs) are formed between DEX and the protein. The 3′-carbonyl oxygen in the A ring HBs to the guanidinium group of Arg611 and to the γ-amide group of Gln570. On the D ring, the 17-β-hydroxyl group interacts with Gln642 while the 21-carbonyl HBs with Thr739. The 11-hydroxyl in the C ring and the 24-hydroxyl in the D ring can interact with Asn654. Additionally, significant vdW contacts can be made with Leu753, Ile747, and Phe749.

As extensively reviewed in the literature,[1,7,8] glucocorticoids (GCs) are widely used to treat a variety of inflammatory and immune diseases such as asthma and allergy conditions. The first GCs to be discovered such as cortisol or DEX still represent the main treatment for conditions of the inflammatory process despite the fact that they carry a significant risk of side effects. The understanding that trans-activation and trans-repression are distinct mechanisms activated by the ligand−protein complex focused scientific research on the identification of "modulators" of the glucocorticoid receptor aiming to separate therapeutic requirements from side effects. Intensive research to date has delivered a wide set of GR-binders with a large variety of biological profiles which can readily be exploited through ligand-based drug design (LBDD).[3]

Molecular modeling has gained a key role in the process of drug discovery with many tools now available among which virtual screening (VS) is well-known. VS approaches are implemented for examining large compound databases in silico and for identifying a selected number of molecules for in vitro testing. VS can be divided typically in two categories: ligand-based and structure-based drug design (SBDD). In LBDD, properties and features of known ligands are used to retrieve novel biologically effective compounds. In SBDD, a more detailed knowledge of the target protein is required.[9,10] This information is directly used for the retrieval or design of novel molecules considering the receptor/target coordinates. Various LBDD and SBDD approaches have been applied to

*To whom correspondence should be addressed. Phone: 353-1-8961634. Fax: 353-1-6762400. E-mail: david.lloyd@tcd.ie.

[a] Abbreviations: GR, glucocorticoid receptor; LBD, ligand binding domain; LBDD, ligand-based drug design; FP, fluorescence polarization; TR, trans-repression; TA, trans-activation; DBD, DNA binding domain; AF-2, activation function domain 2; DEX, dexamethasone; GC, glucocorticoid; VS, virtual screening; SBDD, structure-based drug design; World of Molecular Bioactivity, WOMBAT.

Published on Web 03/24/2010

the GR and discussed in the literature and have been recently reviewed. To date only limited structure-based design approaches have been reported in the literature.[11,12]

In this work, we report the first application, to our knowledge, of a "classical" LBDD computational strategy consisting of pharmacophore building, validation, and database screening (using Catalyst[13]) to the identification of novel nonsteroidal GR modulators.

Results

A collection of 106 compounds was gathered from the literature and classified as GR modulators with different profiles in trans-activation (TA) or trans-repression (TR). The training set for pharmacophore development was chosen according to the Catalyst guidelines based on high activity, selectivity, and chemical diversity. From the full data set, 19 molecules, including steroidal and nonsteroidal structures, were selected as the **training set** with affinity values ranging over approximately 4 orders of magnitude, between 0.1 nM for structure **1** and 4.1 μM for structure **19** (Table 1, Supporting Information). The K_i values retrieved from radioligand binding assays in which [H^3]DEX was displaced by other drugs in a concentration-dependent fashion were utilized to determine the relevance of the pharmacophore in the ensemble. The training set selected was representative of most of the known GC modulators and the individual pharmacophore in the ensemble is therefore thought to capture the essential features responsible for the biological activity. The molecules are approximately evenly distributed among each order of magnitude.

HypoGen Pharmacophore. Typically, the pharmacophore identification process supported in the Catalyst environment involves 3D structure generation, conformational exploration, and definition of the pharmacophore features consistent with the generated training set. When working with legacy Catalyst generated pharmacophores, it is important to keep in mind that the version of Catalyst has a strong influence on the developed pharmacophore.

In developing the best pharmacophore hypothesis from the training set, a number of different sets of hypotheses were generated, each containing 10 pharmacophores, and the best ranked hypothesis of each set were compared through analysis of statistical parameters. A full list of relevant parameters regarding the best hypothesis selected is presented in the Supporting Information. The pharmacophore hypothesis selected included a hydrogen bond donor, a hydrophobic feature, a hydrophobic aliphatic feature, and a ring aromatic feature. The null cost and fixed cost were equal to 146 and 78, respectively, with a difference of 68. The fixed cost is the cost of a perfect hypothesis able to exactly match predicted to experimentally determined activity. The null cost is the cost of a hypothesis that gives no correlation between the predicted activity and the experiment activity. The fixed cost and null cost represent the upper and the lower bound, respectively, and the difference between the two costs indicates the statistical significance of the run. The current value of 68 bits is within the appropriate range. The configuration cost describing the complexity of the hypotheses space is 13 and therefore acceptable. These experimental configuration values equate to Catalyst evaluating 8192 hypotheses which were able to discriminate between active and inactive molecules. The best 10 hypotheses were selected for assessment.

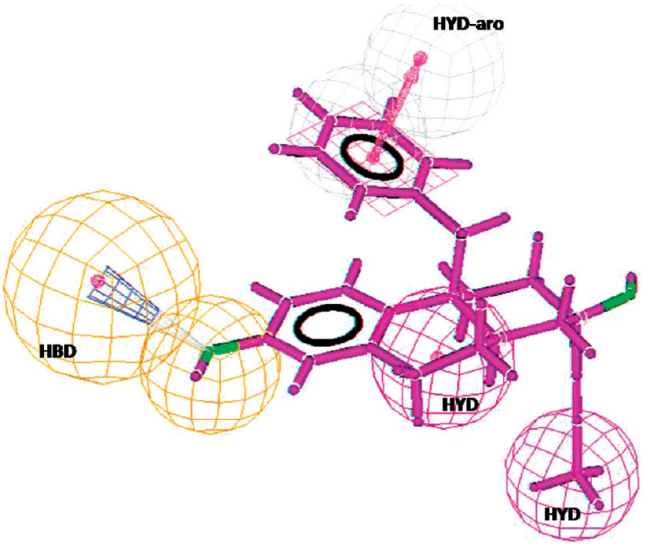

Figure 1. Pharmacophore fitting of **2** to hypothesis 1. HBD: hydrogen bond donor; HYD: hydrophobic; HYD-aro: hydrophobic aromatic. The predicted activity was 0.067 nM.

The robustness of this model was assessed through analysis of the correlation coefficient $R^2 = 0.92$ and the root-mean-square deviation of affinity data rmsd = 1.18. Four compounds in the training set showed a deviation between experimental and predicted affinity values in the order of 3-fold higher experimental versus predicted. We deemed these exceptions tolerable in the search for novel "hit" molecules and noted that the second most active compound in the training set 4a(*S*)-Benzyl-2(*R*)-prop-1-ynyl-1,2,3,4,4a,9,10,10a(*R*)-octahydro-phenanthrene-2,7-diol **2** (CP-409069)[18−23] was able to map directly to all the pharmacophoric elements of the model (Figure 1). Through the model overlay, the phenol oxygen matched the hydrogen bond donor feature, whereas the benzyl ring on the side chain mapped the aromatic ring feature. The methyl substituent on the alkyne side chain and the central saturated ring match the hydrophobic features. In such an orientation, the computationally predicted affinity of 0.067 nM was in very good agreement with the measured experimental value of 0.17 nM. The strong biological potency of this molecule suggested that it possesses many or all of the molecular features required for affinity and effective hGR modulation and that, moreover, the pharmacophore model correctly estimated all the features necessary for the major interactions between **2** and the receptor.

Validation Set. A **validation set** was processed in a similar way to the training set and contained 87 active molecules distributed among 913 decoys. The decoy set was selected from the World Drug Index (WDI).[14] Using our established methodology for database prepreparation,[15] filtering was applied to remove compounds with intrinsically non-lead-like properties.[16] In brief, a focused decoy set of 1000 compounds was selected from the World of Molecular Bioactivity (WOMBAT) database. OpenEye's FILTER was applied by removing compounds with intrinsically non-lead-like properties such as those with molecular weights ≤ 200 or > 550, the number of hydrogen bond donors $0 < x > 10$, and calculated log P values < 7. Subsequently, a Perl script was used to select a random subset of compounds from this filtered data set. Over half of all known marketed drugs contain chiral centers, and it was deemed of importance to represent this in the data set. To this end, 500 molecules with

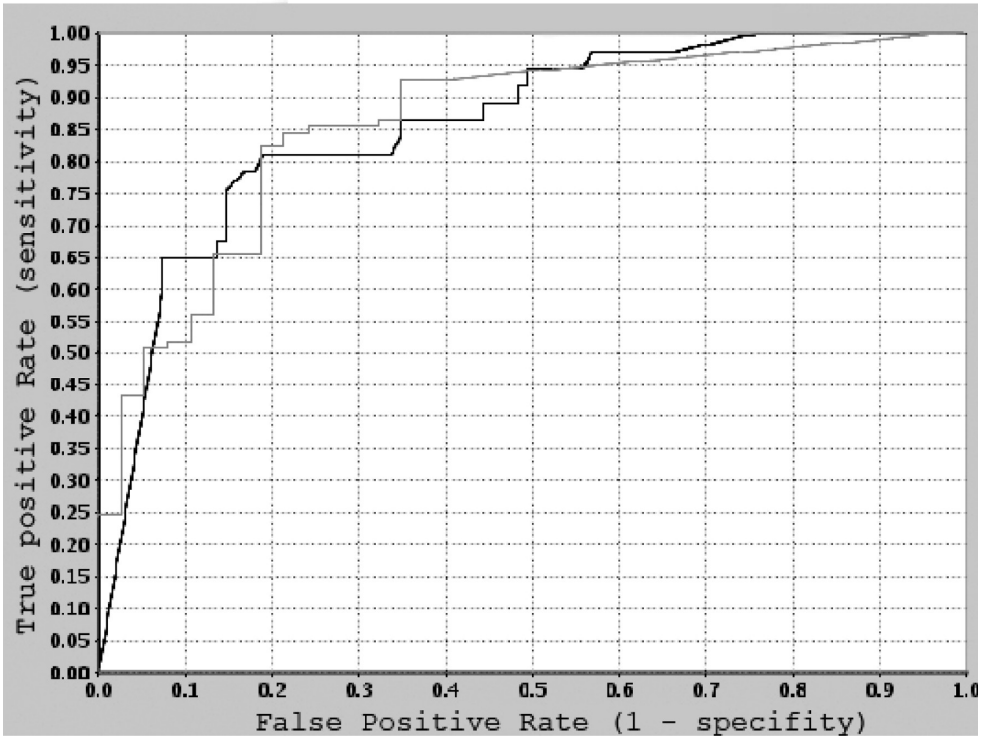

Figure 2. ROC curves calculated in Pipeline Pilot after the screening of the validation set through hypothesis 1 without a shape constraint (black line: accuracy 0.858) and with a shape refinement (gray line: accuracy 0.856).

their specific, active, chiral, and isomeric data were taken from the WDI using the Daylight toolkit. Subsequently, 460 molecules whose active chirality and isomers were unspecified or ambiguous were also selected and added to the data set. This prevented any sources of imbalanced results where the decoy compounds are not representative of active species. The data set was retained in SMILES format.

As the statistical parameters did not provide enough standalone information to fully evaluate the predictive power of the pharmacophore models, a screening of the validation set was performed using the Best Flexible Search implementation in Catalyst. The corresponding ROC curve was calculated using Pipeline Pilot[27] and is shown in Figure 2.

The model selected successfully returned 59 out of 87 seeded active molecules, along with 113 decoys across a total of 1000 molecules originally included in the data set. A strong point of this model is that it was able to accommodate and identify a diverse variety of known modulator structures. The retrieved active molecules were representative of different categories of GR modulators. However, among the steroid structures, only the antagonist **3**[18] (RU-486) was able to pass the filter. This was deemed acceptable as our objective was the identification of novel nonsteroidal modulators.[19−23] The ROC curve has a final score of 0.86, indicating this to be a predictive model and that most active molecules that passed were ranked better than the decoys.

To visualize how the pharmacophore query was related to the physiological protein binding pocket, the crystal structure 1M2Z[4] was used as a frame of reference and the Catalyst hypothesis was imported into the MOE environment.[28] For illustrative purposes, we present the mapping of the compound ID **20**[29] structure (Figure 3) as performed by Catalyst and the imported pharmacophore overlaid on the docked conformer of structure **20** into the 1M2Z protein structure (Figure 3; docking performed using FRED[30]).

In this mapping, the hydrogen bond donor is matched by the ligand oxygen in the propanol side chain and projects toward Gly567 and Met565, which are within a distance to engage in hydrogen bond interactions. The hydrophobic feature is perfectly matched by one of the aromatic rings, and its projection is directed toward the hydrophobic residues Leu608 and Phe623. The second hydrophobic feature is matched by the dimethyl substituents on the dihydro-pyridine ring, and it faces the phenyl ring of Tyr735. Finally, the hydrophobic aliphatic feature matches the methyl substituent on the dihydro-pyridine ring on structure **20**.

This analysis was performed in order to examine the interrelationship between the generated pharmacophore and a ligand docked within the GR ligand binding pocket. A good mapping of features, amino acids, and ligand positions was observed.

Shape Refinement. It is likely that a pharmacophore query with no spatial constraint will returns hits that are too voluminous to fit into the ligand binding site when used in a VS procedure. In employing ligand-based models, spatial information can be derived from known active ligands by fitting large and rigid compounds into the model and converting the molecule into a shape query. The derived shape is then merged with the initial hypothesis to become an integral part of the pharmacophore query. Compounds unable to conform to the shape query are then discarded.

As a spatial refinement for the GR modulators, the rigid compound **20** was fitted into the initial hypothesis and converted into a shape query. Structure **20** was chosen as the shape query for its ability to map the pharmacophore features and fit within the hGR binding site as found from the docking analysis. To test the potential of the refined hypothesis, the validation set was rescreened using the Best Flexible Search algorithm. On inclusion of a shape query constraint, about 7% of the validation set passed the pharmacophore

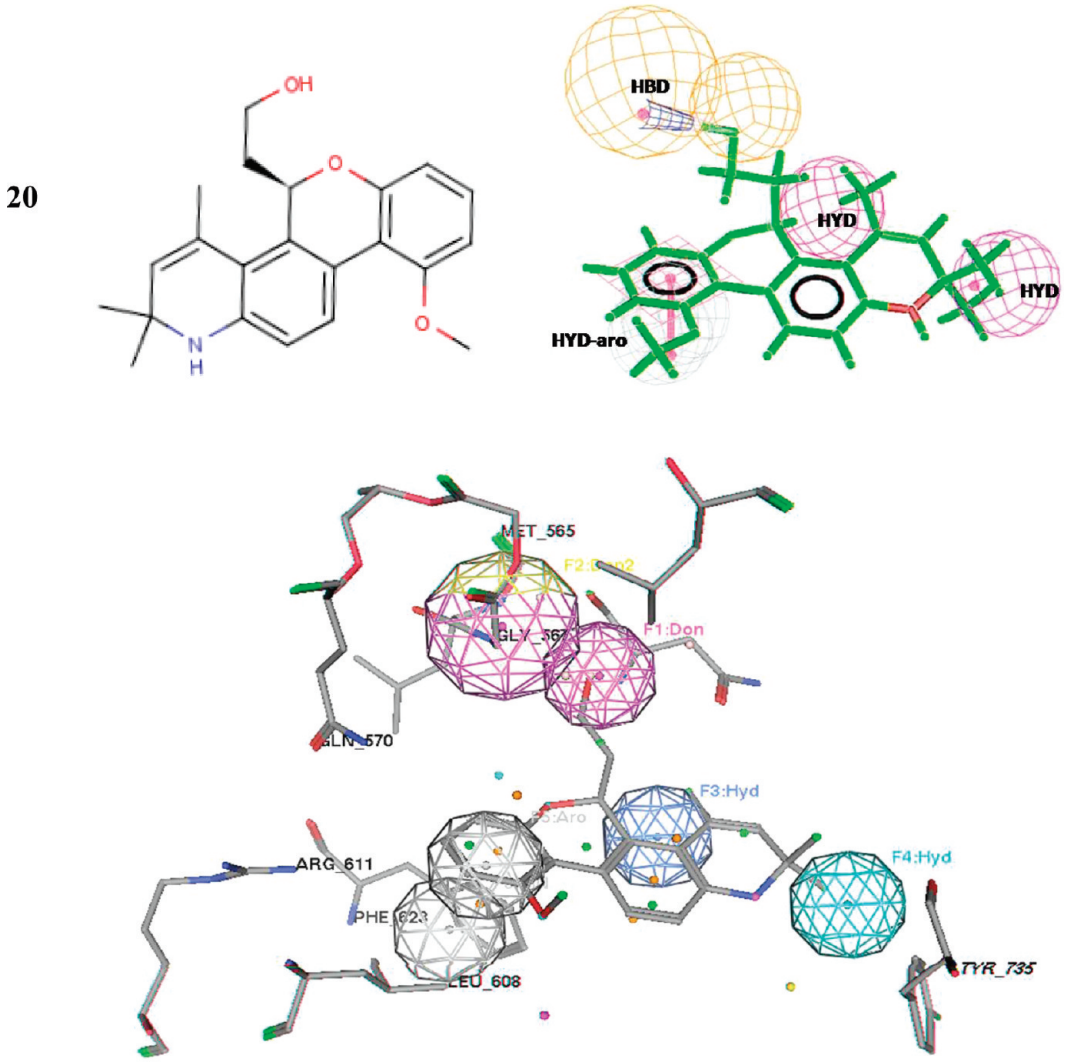

Figure 3. Pharmacophore mapping of compound ID **20** performed by a Catalyst Flexible Best Search. This mapping was used as a reference for the MOE environment pharmacophore mapping. The yellow spheres represent the hydrogen bond donor feature and its projection. The gray spheres represent the aromatic ring feature and its projection, and the pink spheres are the hydrophobic features. In the lower image, hypothesis 1 was imported into the MOE environment and overlaid on the docked conformation of compound **20** in the 1M2Z crystal structure. Some of the relevant residues are displayed in the picture. Feature labels are shown in the figure.

filter with 39, of which were known GR modulators. A ROC curve (Figure 2) was calculated, and a score of 0.85 was again obtained. The "exclusion" of 20 active compounds was mainly confined to the more poorly ranked molecules of the set which would not typically be sourced subsequent to the validation stage of a VS protocol (i.e., validation tends to be executed on the top ranked "hits"). The ROC curve shows that the performance of the shape-refined hypothesis is highly sensitive in discriminating actives from inactives.

Screening Data Set. Three commercial vendor databases (Asinex Platinum,[31] Peakdale,[32] and Specs[33]) were merged to yield a total screening set of 264000 compounds. Two-dimensional (2D) structures were input to CORINA to generate one single conformer for each molecule. The structures were then converted into .bdb format through the *CatSD* implementation before being imported into Catalyst. Multiple conformers were then generated using the BEST enumeration algorithm. Molecules were stored in a Catalyst database and screened through the shape-refined hypothesis using the Best Flexible Search implementation supported in Catalyst. The pharmacophore output list contained 717 molecules which were docked into the GR crystal structure (PDB: 1M2Z) using FRED.[30] The best ranked molecules from the pharmacophore output were visually inspected, and their docking poses and diversity guided the selection of 11 compounds for examination in an in vitro fluorescence polarization assay.

Biological Results

Hits Identified. All 11 selected molecules were assayed in vitro at a single concentration of 10 μM in triplicate in a FP competitive binding assay. Two molecules, (Figure 4) **21** (MDG169) and **22** (MDG199), in-house numbering scheme, bound to the hGR, demonstrating the successful utility of this VS method.

21 and **22** were initially evaluated for their ability to bind the hGR at 10 μM in a competitive FP binding assay. **21** caused a reduction of the mP value of 65% compared to the vehicle, while DEX reached 87% at 1 μM.

The mP reduction caused by **22** at 10 μM was ~50% of the vehicle mP value, while DEX reached 87% reduction at 1 μM. On the basis of the single point potency, we selected

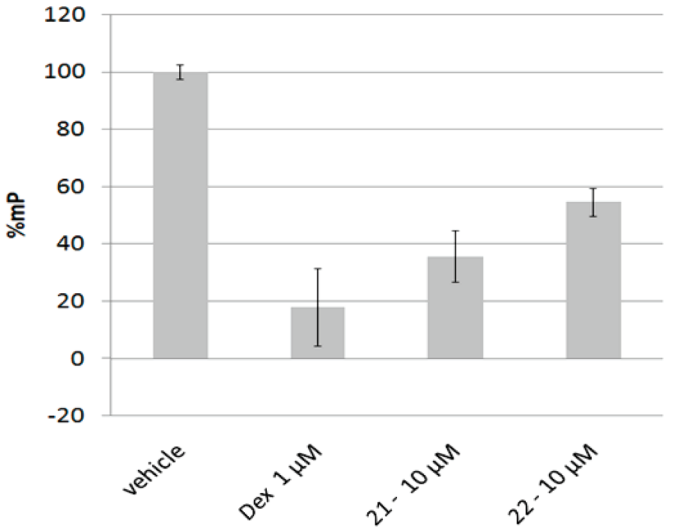

ID	Structure
21	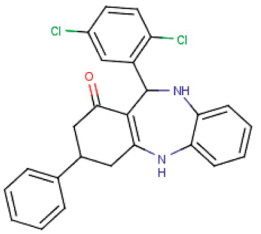
22	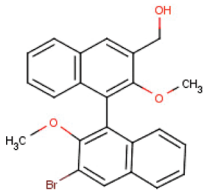

Figure 4. Successful hGR-binders retrieved from pharmacophore search. (A) **21** structure. (B) **22** structure. Molecules retrieved by virtual screening procedures demonstrating binding to hGR by FP assay.

21 for a full dose−response experiment and for further biological evaluation (Figure 5).

The experimental IC_{50} for DEX was calculated to be 11.24 ± 0.93 nM (with an experimental value of 11.4 nM from the Invitrogen kit), while for **21** it was calculated to be 2.41 ± 0.22 μM—validating the scaffold as a new nonsteroidal molecular probe for this target. The potency of **21** was computationally estimated to be between 0.9 and 79 μM according to the range of pharmacophore mapping, with the molecule being well contained within the shape constraint.

To assess the selectivity of the pharmacophore model, the molecule was subsequently tested for its potential cross-reactivity with other nuclear receptors. **21** caused no reduction of the FP mP value in on-target assay at 50 μM for recombinant human ERα, ERβ, and PPARγ. Accordingly, we conclude that this molecule selectively binds to the hGR over these receptors (data not presented).

To aid future lead optimization studies, we next investigated the binding mode of **21**. By default, Catalyst offers

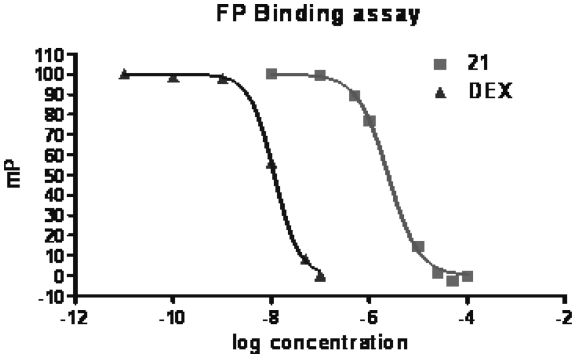

Figure 5. FP binding assay of **21** and DEX on hGR. The displacement of fluorescent molecule with increasing concentrations of competitor that results in a half-maximum shift polarization equals the IC_{50} of the competitor. Each point is the result of triplicate samples. Error bars are shown.

a range of possible mappings of the molecule to the pharmacophore query, and for each mapping an estimated activity is

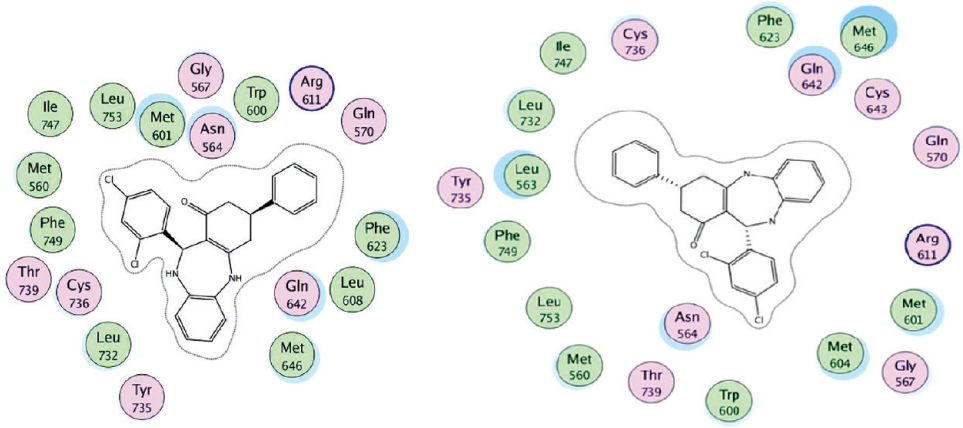

Figure 6. Ligand−protein interaction plots calculated in MOE for the binding poses retrieved by docking **21** into 1M2Z.

assigned. **21** contains two chiral centers with undetermined chirality in the binding mode (and unqualified by the commercial vendor). In Catalyst, when chiral centers are set as unknown, the program uses mirror images during the conformational search, exploring all possible combinations. Given a general agreement of the poses, the final choice of the most feasible mapping was guided by the comparison with docking results. Docking was performed using FRED (Chemgauss2 scoring function) to fit conformers exported from Catalyst into the 1M2Z crystal structure. From the docking poses, two main modes were retrieved. In the first model, the phenyl ring behaves as an A ring mimetic directed toward Arg611 and Gln570. The dichlorophenyl ring is oriented toward helix 11−12 overlaying on the C-17 side chain of the DEX structure. The rest of the dibenzo-1,4-diazepin core partially covers the steroid structure, with the keto group of the diazepin core being close to O-11 of the DEX structure and therefore being potentially able to engage in similar hydrogen bond interactions (Figure 6 left). In this conformation, the chiral center of the 2,4-dichlorebenzyl is in *R* configuration, while the chiral center of the benzyl ring is in the *S* configuration. The second binding mode (Figure 6 right) retrieved from the docking experiments has the unsaturated ring of the dibenzo-1,4-diazepin core mimicking the A ring of the steroid structure. The 2,4-dichlorobenzyl is perpendicular to the plane identified by the dibenzo-1,4-diazepin scaffold and is directed toward Leu753 and Asn564. From the crystal structure of the antagonist mode, it was observed that this part of the binding pocket is occupied by the dimethylaniline side chain of **3**, which is responsible for the antagonist arrangement of helix12. In this conformation, the chiral center of the 2,4-dichlorobenzyl is in an *S* configuration while the chiral center of the benzyl ring is in the *R* configuration.

Docking was performed using FRED to fit conformers exported from Catalyst into the 1M2Z[4] crystal structure. For comparison, the binding mode is superimposed onto the cocrystallized DEX. In the **21** binding mode, the phenyl ring behaves as a steroid A ring mimetic directed toward Arg611 and Gln570. The dichlorophenyl ring is oriented toward helix 11−12 overlaying on the C-17 side chain of the DEX structure. The rest of the dibenzo-1,4-diazepin core partially covers the steroid structure with the keto group of the diazepin core being close to O-11 of the DEX structure and therefore being potentially able to engage in similar hydrogen bond interactions. The hydrogen bond donor feature is mapped by the nitrogen atom on the dibenzo-1,4-diazepin ring, in good agreement with the docking result (Figure 7B) and the pharmacophore orientation within the binding pocket.

To illustrate a direct comparison between the second most active ligand (**2**) and **21**, the highest ranked docked pose of each compound were overlaid on each other. The overlay was achieved by mapping the protein backbones onto each other so as to display commonalities between the bound ligands' orientations. A high degree of spatial occupancy and structural similarity can be observed between both compounds as illustrated in Figure 8.

Trans-Repression Assay. The trans-repression (TR) potential of **21** was evaluated by its ability to inhibit the production of IL-1-induced, IL-6 expression in the human A549 lung epithelial cell line. This inhibition has been shown to be GR-mediated at the transcriptional level, and because conventional GCs are known to repress IL-6 production in the system, monitoring IL-6 inhibition by this method provides a direct immunologically relevant means for evaluating our novel GR ligands for trans-repression activity.[34] The treatment of A549 cells with DEX inhibits the production of IL-1-induced IL-6 in a dose dependent manner. Treatment of the A549 cells with **21** alone at 10 μM showed no inhibitory effect on the expression of IL-6 (Figure 9).

Co-treatment of A549 with **21** (10 μM) in combination with DEX showed an improved inhibitory effect when compared to DEX alone (Figure 10). Moreover, this cooperative effect was dependent on the DEX dose with a higher extent of inhibition at 1 nM DEX in combination with **21** (10 μM), showing a ~70% improvement when compared to 1 nM DEX alone.

Discussion

There is an ongoing need to find GR modulators that preserve the immune effects of GRs without the detrimental side effects. Rational design approaches are used to accelerate the discovery of such new chemical entities toward becoming new drugs. This work represents the first utility of a pharmacophore model in a vHTS to identify novel nonsteroidal hGR modulators. We contend that the single biggest limitation of ligand-based drug design approaches continues to be the available data set. Ideally, a data set containing feature-poor compounds with diverse structures and similar validated activities for a given target would greatly improve the utility and results of such ligand-based methodology. Approaches

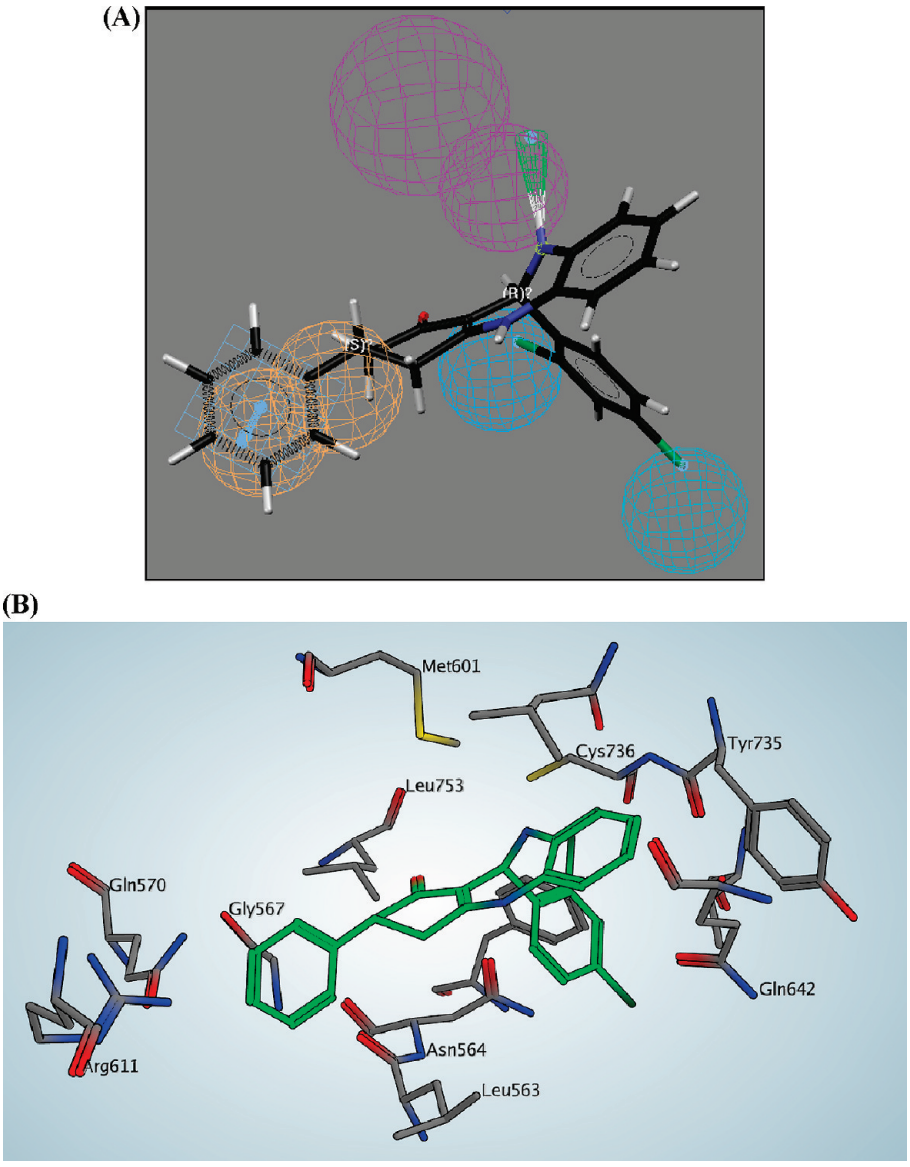

Figure 7. (A) Mapping of **21** onto the Catalyst pharmacophore. The estimated activity of this pharmacophore mapping is ~79 μM. (B) The first binding mode of **21** within the hGR-LBD obtained from docking.

such as that presented here for pharmacophore generation can be additionally challenging when the molecules employed for model construction are structurally distinct from the available data set of experimentally cocrystallized target ligands, particularly in terms of generating ligand alignments and pose validations.

Challenges aside, the model described embodies the key pharmacophoric features required for receptor binding and was mapped successfully into the receptor—relating each pharmacophore feature to the residues within the binding site. Application of the pharmacophore as a query for virtual screening completed its validation. The model selected with its optimum predictive power as demonstrated by the ROCs curves was directly applicable to guide the virtual screening procedure outlined.

The encouraging in silico results obtained were fully validated through in vitro assay, furnishing two novel nonsteroidal compounds exhibiting low μM on-target affinity and hGR selectivity over other human nuclear receptors; a more detailed selectivity profile involving the mineralcorticoid receptor, androgen receptor, progesterone receptor, and other members of the nuclear receptor family will be advanced in due course. An examination of the binding modes predicted for **21** demonstrates a good overlay for this novel nonsteroidal ligand with the DEX steroidal cocrystal structure. Of the two

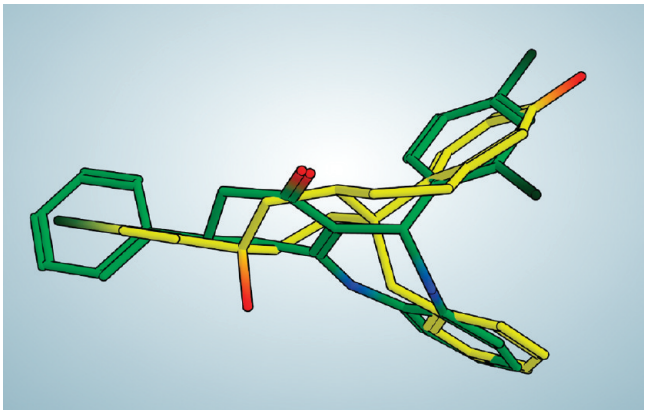

Figure 8. Overlay of **2** (yellow) and **21** (green) illustrating the structural similarities between the new hit compound and a known active.

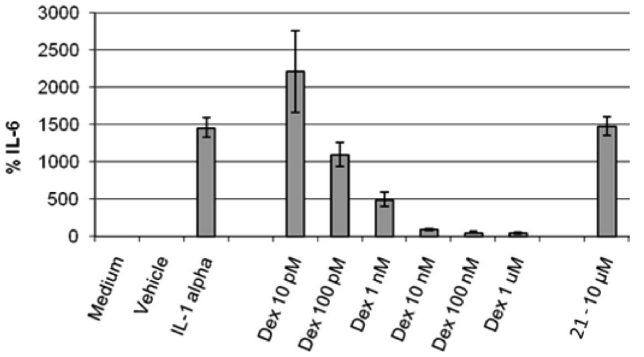

Figure 9. Trans-repression results for a single point concentration of **21** at 10 μM. A549 cells were stimulated with IL-1 at 10 ng/mL. The *y* axis measures the expression of IL-6 as a percentage of its expression after A549 stimulation with IL-1α.

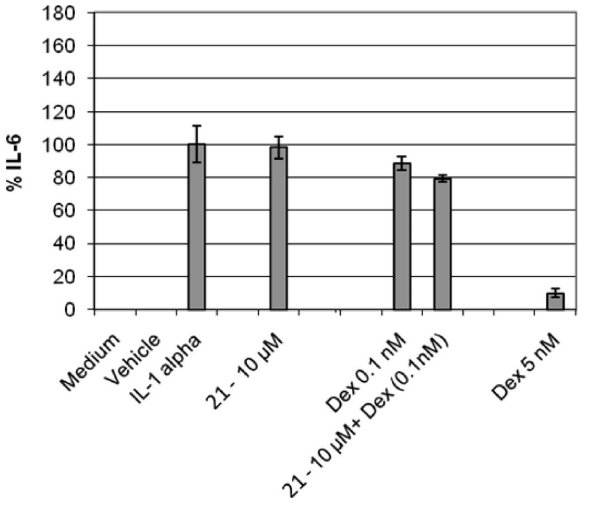

Figure 10. Trans-repression result for a single point concentration of **21** at 10 μM and in combination with different DEX concentrations. A549 cells were stimulated with IL-1 at 10 ng/mL. The *y* axis measures the expression of IL-6 as a percentage of its expression after A549 stimulation with IL-1α.

hits identified from our predictive pharmacophore screen, **21** was deemed the more viable molecular probe and advanced to additional mechanistic cell-based studies.

To measure the similarity between **21** and **22** and known GR modulators, 140 known GR modulators (including both the validation and the training set) were selected from the literature. MDL public keys and functional-class fingerprints (FCFP4) were calculated as implemented in Pipeline Pilot and a similarity analysis was performed using the Tanimoto coefficient. FCFPs are a type of extended-connectivity fingerprints that use a functional-class atom typing scheme (e.g., donor, acceptor etc.), and MDL public keys are a set of 166 mostly substructural features. Table 1 outlines the maximum similarity coefficients for **21** and **22**, highlighting their diversity from known GR modulators and novelty as GR chemotypes.

In the search for GR modulators the aim is to separate the beneficial anti-inflammatory effects, derived from TR pathways, from the side effects derived from TA pathways. Hence, the ability of the compounds to inhibit the production of IL-1-induced IL-6 expression in the human A549 lung epithelial cell line was further examined. The cotreatment of A549 with **21** (10 μM) in combination with DEX showed an improved inhibitory effect when compared to DEX alone.

Table 1. Structural Similarity between the Two Hit Compounds and Known GR Modulators

	MDL fingerprint	FCFP 4
21	0.51666	0.30909
22	0.54545	0.29231

The cooperative effect was also dependent on the DEX dose with a higher extent of inhibition at 1 nM DEX in combination with **21** (10 μM), showing a ~70% improvement when compared to 1 nM DEX alone. The enhanced IL-6 inhibition caused by the cotreatment of A549 cells with DEX and **21** necessitates an investigation of the drug diffusion through the cell membrane and the internal cell signals involved.

In moving from a hit to a lead compound, two different rounds of substitutions around the identified hit compound, **21**, are envisaged. First, the dichlorobenzyl ring directed toward helix11−12 could be chemically explored with the introduction of polar groups such as a hydroxyl, a methyl acetate, a methyl ester, and nitro groups. These polar groups could be able to act as the O-11 on the steroid structure engaging in hydrophilic interactions with key residues such as Thr739, Cys736, or with Asn564 on helix3. Furthermore, it is postulated that heterocycles of five- or six-member rings could favor the formation of an interaction with less bulky substituents, thereby minimizing the steric clashes. Hydrophobic substitutions on the benzyl ring such as *p*-methyl could help to design a more complete picture. A second round of substitutions could involve the benzyl ring directed toward Arg611 and Gln570. Electronegative, polar, hydrophobic, and five-member rings could all be investigated to optimize the interactions with the protein residues. The introduction of hydrophilic groups in the para and meta position should be able to mimic the O-3 on the A-ring of the steroid core and enhance the binding affinity. These chemical enhancements and the investigation of different substituents in the para and meta positions of the aromatic cores will be explored in future work.

The recent availability of novel hGR LBD crystal structures, some with larger binding pockets, will undoubtedly have a marked impact on future rational drug design for GR modulators. We designed a pharmacophore based on a diverse selection of GR modulators. Our objective in this work was to scaffold-hop away from existing chemotypes into previously unexplored regions of chemical space. With that in mind, the pharmacophore presented has utility for lead finding, as opposed to lead optimization. When sufficient additional biological data has been generated on a chemical series based around this scaffold anticipate development a focused pharmacophore to guide further lead optimization studies.

Methods

General Procedures. All compounds were commercially available and purchased from Specs. Purities of compounds were determined by a combination of ^{1}H NMR and MS and were found to be >95%.

Computational Methods. Conformer Generation. Once the active data set (Table 1, Supporting Information) was collected, a default conformational search was performed to increase the likelihood that bioactive ligand conformations are embodied in the pharmacophore analysis. The training set was input to CORINA[17] to generate single 3D structures which were then imported into Catalyst. Conformational ensembles of each compound were generated with CatConf Fast to sample bioactive conformational space. The molecules and their correlated conformations were stored as a Catalyst database.

Pharmacophore Generation. The HypoGen implementation in Catalyst uses activity values (K_i or IC_{50}) to derive hypotheses rationalizing the trends of activity observed within the training set. After tuning the feature selection, pharmacophore models were built to include hydrogen bond acceptor (HBA), hydrogen bond donor (HBD), aliphatic hydrophobic, hydrophobic aromatic, and ring aromatic as possible features. Because of the molecular flexibility and functional complexity of the training set, only pharmacophores containing four or more features were considered by setting the *MinPoints* flag to 4. The *Spacing* (minimum interfeature spacing allowed in a hypothesis) value was decreased from 297 to 150 picometers.

As a pharmacophore analysis produces several hypotheses, there is a clear need to identify those models with biological and statistical relevance. A common way to validate a model is to test its ability to identify active molecules seeded in a larger set of decoys (*validation* or *test set*). This ability can be quantified through receiver operating characteristic (ROC) curve and statistical analyses of the data. The overriding principle of our research group, however, is that only in vitro testing of the identified hits can demonstrate the quality of a VS method.

ROC Analysis. A common method for distinguishing the significance of a hypothesis is to evaluate how the model discriminates between active molecules and the decoy set. In a ROC curve, the true positive rate is plotted as a function of the false positive rate. Each point on the ROC curve represents a sensitivity/specificity pair. An ideal test with perfect discrimination (no overlap in the two distributions) has a ROC plot that passes through the upper left corner (100% sensitivity, 100% specificity).

Docking. Conformers were generated using the Omega software from OpenEye and docking was performed using Fred v2.1.2. FRED performs an exhaustive docking by enumerating rigid rotations and translations of each given conformer within the active site with a series of filters, then rejecting poses that do not have sufficient shape complementarity to the protein's active site. The conformers were generated with Corina[17] and subsequently with Omega[24] (upper limit 100 p/m, Energy Window 20 kcal/mol and rmsd cutoff 0.8 Å). The optimized poses were scored by multiple scoring functions, and for each scoring function, a ranked list was returned. Each pose was then assigned a consensus score equal to the average of the poses ranked in each list (rank by rank).

Statistical Evaluation and Refinement of the Pharmacophore Hypothesis. Multiple hypotheses were evaluated according to the Catalyst guidelines. The pharmacophore query was utilized to screen the validation set containing a collection of 87 actives seeded in 913 decoys. A ROC curve was calculated for each output to evaluate the ability of any given model to discriminate between active and decoy sets. The pharmacophore query was further refined through a shape-based methodology supported in Catalyst. The refinement step delivered a new hypothesis with the shape constraints being an integral part of the original query. The refined model was then retested on the validation set.

Biological Methods. Fluorescent Polarization. A fluorescence polarization (FP) competition binding assay was performed as indicated by the supplier Invitrogen.[25] In a 96-well fluorescence plate, additions to each well were prepared as follows: 1 μL of test compound at the desired concentration was first added and immediately mixed with 49 μL of Complete GR screening buffer. Then 25 μL of hGR-LBD solution (0.016 pmol/μL) and 25 μL of 4 nM solution of Fluoromone were added for a total volume of 100 μL. The plate was allowed to incubate in the dark for 2 h at room temperature. Plates were read using a PHERAstar Plus HTS microplate reader, and the results were analyzed using Graph Pad Prism.[26] A vehicle control contained 1% DMSO (v/v). Negative and positive controls were always included in the plates. The negative control contained 50 μL of complete GR screening buffer, 25 μL of 4 nM solution of Fluoromone, and 25 μL of 0.016 solution of GR. This control was used to determine the polarization value when no competitor was present (theoretical maximum polarization). The positive control is identical to the negative control but includes 1 μL of DEX (at the desired concentration). This well represents 100% competition on the test reaction. The reading was performed with 485 nm excitation and 530 nm emission interference filters. As the aim of the study is to compare the relative affinities of a series of ligands, through IC_{50} values, identical conditions were used in all the experiments.

Trans-Repression Study. A549 (carcinomic human alveolar basal epithelial cells) cells were cultured at 37 °C in DMEM medium and 10% of FCS. Cells were seeded at a concentration of 5×10^4 cells/well in a 96-well plate and incubated at 37 °C in 10% CO_2. After 24 h, the medium was removed and replaced with serum-free media. Cells were serum-starved for 72 h. Where appropriate, cells were pretreated with DEX (1 nM) or GR compounds (10 μm) 2 h before IL-1 addition (10 ng/mL). After 24 h incubation at 37 °C, the supernatant was removed and stored at −20 °C until ready for ELISA analysis.

Acknowledgment. We sincerely thank the software vendors for their continuing support for such academic research efforts, in particular contributions from OpenEye Scientific, Scitegic, Accelrys, and Chemical Computing Group. This work was financially supported through funding from Science Foundation Ireland, Cancer Research Ireland, and Enterprise Ireland.

Supporting Information Available: Pharmacophore training data set and HypoGen pharmacophore details. This material is available free of charge via the Internet at http://pubs.acs.org.

References

(1) Buckbinder, L.; Robinson, R. P. The glucocorticoid receptor: molecular mechanism and new therapeutic opportunities. *Curr. Drug Targets Inflammation Allergy* **2002**, *1* (2), 127–136.
(2) Kumar, R.; Thompson, E. B. Transactivation functions of the N-terminal domains of nuclear hormone receptors: protein folding and coactivator interactions. *Mol. Endocrinol.* **2003**, *17* (1), 1–10.
(3) Coghlan, M. J.; Elmore, S. W.; Kym, P. R.; Kort, M. E. The pursuit of differentiated ligands for the glucocorticoid receptor. *Curr. Top. Med. Chem.* **2003**, *3* (14), 1617–1635.
(4) Bledsoe, R. K.; Montana, V. G.; Stanley, T. B.; Delves, C. J.; Apolito, C. J.; McKee, AD. D.; Consler, T. G.; Parks, D. J.; Stewart, E. L.; Willson, T. M.; Lambert, M. H.; Moore, J. T.; Pearce, K. H.; Xu, H. E. Crystal structure of the glucocorticoid receptor ligand binding domain reveals a novel mode of receptor dimerization and coactivator recognition. *Cell* **2002**, *110* (1), 93–105.
(5) Sack, F. U.; Reidenbach, B.; Dollner, R.; Schledt, A.; Gebhard, M. M.; Hagl, S. Influence of steroids on microvascular perfusion injury of the bowel induced by extracorporeal circulation. *Ann. Thorac. Surg.* **2001**, *72* (4), 1321–1326.
(6) Williams, S. P.; Sigler, P. B. Atomic structure of progesterone complexed with its receptor. *Nature* **1998**, *393* (6683), 392–396.
(7) Schacke, H.; Docke, W. D.; Asadullah, K. Mechanisms involved in the side effects of glucocorticoids. *Pharmacol. Ther.* **2002**, *96* (1), 23–43.
(8) Schacke, H.; Schottelius, A.; Docke, W. D.; Strehlke, P.; Jaroch, S.; Schmees, N.; Rehwinkel, H.; Hennekes, H.; Asadullah, K. Dissociation of transactivation from transrepression by a selective glucocorticoid receptor agonist leads to separation of therapeutic effects from side effects. *Proc. Natl. Acad. Sci. U.S.A* **2004**, *101* (1), 227–232.
(9) Gubernator, K, Böhm, H.-J., Eds. *Structure-Based Ligand Design*; Wiley-VCH Verlag GmbH: Weinheim, 1998; Vol. 6, pp xiv, 153.
(10) Lyne, P. D. Structure-based virtual screening: an overview. *Drug Discovery Today* **2002**, *7* (20), 1047–1055.
(11) Onnis, V.; Kinsella, G.; Carta, G.; Fayne, D.; Lloyd, D. Rational ligand-based virtual screening and structure−activity relationship studies in the ligand-binding domain of the glucocorticoid receptor-α. *Future Med. Chem.* **2009**, *1* (3), 483–499.
(12) Onnis, V.; Kinsella, G.; Carta, G.; Fayne, D.; Lloyd, D. Rational structure-based drug design and optimization in the ligand-binding domain of the glucocorticoid receptor-α. *Future Med. Chem.* **2009**, *1* (2), 345–359.

(13) *Catalyst v 4.11*: Accelrys Software Inc.; San Diego, CA, **2005**; http://ir.accelrys.com.
(14) Olah, M.; Mracec, M.; Ostopovici, L.; Rad, R.; Bora, A.; Hadaruga, N.; Olah, I.; Banda, M.; Simon, Z.; Mracec, M.; Oprea, T. I. *WOMBAT: World of Molecular Bioactivity*; Wiley-VCH: New York, 2004; pp 223−239.
(15) Knox, A. J.; Meegan, M. J.; Carta, G.; Lloyd, D. G. Considerations in compound database preparation—"hidden" impact on virtual screening results. *J. Chem. Inf. Model.* **2005**, *45* (6), 1908–1919.
(16) *FILTER*; OpenEye Scientific Software: Santa Fe, NM; www.eyesopen.com, .
(17) *CORINA*; Molecular Networks: Erlangen, Germany; http://www.molecular-networks.com.
(18) Morgan, B. P.; Swick, A. G.; Hargrove, D. M.; LaFlamme, J. A.; Moynihan, M. S.; Carroll, R. S.; Martin, K. A.; Lee, E.; Decosta, D.; Bordner, J. Discovery of potent, nonsteroidal, and highly selective glucocorticoid receptor antagonists. *J. Med. Chem.* **2002**, *45* (12), 2417–2424.
(19) Kym, P. R.; Kort, M. E.; Coghlan, M. J.; Moore, J. L.; Tang, R.; Ratajczyk, J. D.; Larson, D. P.; Elmore, S. W.; Pratt, J. K.; Stashko, M. A.; Falls, H. D.; Lin, C. W.; Nakane, M.; Miller, L.; Tyree, C. M.; Miner, J. N.; Jacobson, P. B.; Wilcox, D. M.; Nguyen, P.; Lane, B. C. Nonsteroidal selective glucocorticoid modulators: the effect of C-10 substitution on receptor selectivity and functional potency of 5-allyl-2,5-dihydro-2,2,4-trimethyl-1*H*-[1]benzopyrano[3,4-*f*]quinolines. *J. Med. Chem.* **2003**, *46* (6), 1016–10130.
(20) Clark, R. D. Glucocorticoid receptor antagonists. *Curr. Top. Med. Chem.* **2008**, *8* (9), 813–838.
(21) Jones, T. R.; Bell, P. A. Glucocorticoid−receptor interactions. Discrimination between glucocorticoid agonists and antagonists by means of receptor-binding kinetics. *Biochem. J.* **1982**, *204* (3), 721–729.
(22) Coghlan, M. J.; Kym, P. R.; Elmore, S. W.; Wang, A. X.; Luly, J. R.; Wilcox, D.; Stashko, M.; Lin, C. W.; Miner, J.; Tyree, C.; Nakane, M.; Jacobson, P.; Lane, B. C. Synthesis and characterization of nonsteroidal ligands for the glucocorticoid receptor: selective quinoline derivatives with prednisolone-equivalent functional activity. *J. Med. Chem.* **2001**, *44* (18), 2879–2885.
(23) Hamann, L. G.; Farmer, L. J.; Johnson, M. G.; Bender, S. L.; Mais, D. E.; Wang, M. W.; Crombie, D.; Goldman, M. E.; Jones, T. K. Synthesis and biological activity of novel nonsteroidal progesterone receptor antagonists based on cyclocymopol monomethyl ether. *J. Med. Chem.* **1996**, *39* (9), 1778–1789.
(24) *OMEGA*; OpenEye Scientific Software: Santa Fe, NM; www.eyesopen.com.
(25) Invitrogen, Polar Screen GR Receptor Competitor Assay Kit, Green, Cat. No. P2816.
(26) *Prism*; GraphPad Software: ; www.graphpad.com.
(27) *Pipeline Pilot*; Accelrys Software Inc.: Santa Fe, NM; http://accelrys.com/products/scitegic.
(28) *MOE, Molecular Operating Environment*; Chemical Computing Group: Montreal.
(29) Elmore, S. W.; Coghlan, M. J.; Anderson, D. D.; Pratt, J. K.; Green, B. E.; Wang, A. X.; Stashko, M. A.; Lin, C. W.; Tyree, C. M.; Miner, J. N.; Jacobson, P. B.; Wilcox, D. M.; Lane, B. C. Nonsteroidal selective glucocorticoid modulators: the effect of C-5 alkyl substitution on the transcriptional activation/repression profile of 2,5-dihydro-10-methoxy-2,2,4-trimethyl-1*H*-[1]benzopyrano[3,4-*f*]quinolines. *J. Med. Chem.* **2001**, *44* (25), 4481–4491.
(30) *FRED*; OpenEye Scientific Software: Santa Fe, NM; www.eyesopen.com.
(31) Asinex Asinexhttp://www.asinex.com.
(32) Peakdale Peakdale Molecularwww.peakdale.co.uk.
(33) SPECS www.specs.net, Specs.
(34) Rosen, J.; Miner, J. N. The search for safer glucocorticoid receptor ligands. *Endocr. Rev.* **2005**, *26* (3), 452–464.